Kinetics of the atrazine degradation process using H$_2$O$_2$-UVC

Sandra M. Sarmento and José T. G. Miranda

ABSTRACT

This work is concerned with the intrinsic reaction kinetic of the degradation of atrazine (ATZ) using H$_2$O$_2$-UVC. Experimental runs were carried out in annular photoreactor. The initial concentration of ATZ was 2.2×10^{-2} mol m^{-3} while the H$_2$O$_2$-ATZ molar ratio range was 0–578 mol H$_2$O$_2$ mol^{-1} ATZ. The ATZ molecules are decomposed by means of free-radical attack (95.2%) and direct photolysis (4.8%). There is an optimal H$_2$O$_2$/ATZ molar ratio ($R_{OP} = 347$ H$_2$O$_2$ mol^{-1} ATZ) which maximizes the initial degradation rate and conversion at 300 s at 83% and 77%, respectively. The process is economically feasible as the values of the energy requirement, energy and H$_2$O$_2$ costs at R_{OP} are 0.14 KWh m^{-3} order^{-1}, US\$0.02 kWh^{-1} m^{-3} and US\$1.0 m^{-3}, respectively. The kinetic model proposed is based on Lea's reaction scheme for the H$_2$O$_2$ direct photolysis, the hypothesis that unknown ATZ sub-products that absorb UVC radiation are generated, and the local volumetric rate of photon absorption. The radiation transport equation was solved and the linear spherical source emission model was used to represent the lamp emission. Intrinsic reaction kinetic parameters were estimated and the model was validated. The model predicted the data in a range of 90 to 98%.

Key words | atrazine, H$_2$O$_2$-UV, kinetics, modelling

Sandra M. Sarmento (corresponding author)
Universidade Federal de Pernambuco,
Departamento de Engenharia Química; Av. Prof. Artur de Sá, SN.,
Cidade Universitária,
CEP: 50740-521,
Recife, PE,
Brazil
E-mail: *sarmento@ufpe.br*

José T. G. Miranda
Refinaria Abreu e Lima; Rodovia PE60,
CEP 55590-000,
Suape, PE,
Brazil

INTRODUCTION

Atrazine (2-chloro-4-(ethylamino)-6-isopropylamino-s-triazine) is the most used herbicide worldwide for pre-emergence and post-emergence control of broad-leaved weeds in several crops, such as sugar-cane, pineapple, maize and sorghum, since its discovery in the 1950s. Atrazine (ATZ) is classified as a priority bio-recalcitrant organic pollutant and an endocrine system disrupter potentially carcinogenic to human beings (Kassinos *et al.* 2009). This herbicide has been used widely in Brazil for about 45 years. The value of the maximum contaminant level in Brazilian drinking water was issued as 2 μg L^{-1} (Brasil Portaria N° 2914 2012).

Direct photolysis is one of the key attenuation processes of ATZ in the environment, as UV radiation breaks down its molecular bonds, thus catalyzing several chemical reactions (Chen *et al.* 2011; Choi *et al.* 2013). However, complete mineralization of ATZ is not achieved in such a process due to the stability of the s-triazine ring toward oxidation (Beltran *et al.* 1996; Chen *et al.* 2011). Advanced oxidation processes (AOPs), such as H$_2$O$_2$-UV, have been used to degrade herbicides by generating free-radicals *in situ*, in particular the hydroxyl radical ($^\bullet$OH). The principal features of the H$_2$O$_2$-UV process

are: (a) free-radicals are generated *in situ* as a result of the direct photolysis of H$_2$O$_2$ at 254 nm; (b) degradation of pollutants can occur by means of synergy of oxidation routes, which are the direct attack of H$_2$O$_2$, direct photolysis at 254 nm, and free-radical attack (Beltran *et al.* 1993; Yue 1993); (c) efficiency process parameters depend on the initial pH, H$_2$O$_2$/pollutant molar ratio as well as on the radiation intensity; (d) the majority of pollutants can be mineralized completely if enough H$_2$O$_2$ is provided and sufficient reaction time is allowed (Alfano *et al.* 2001; Sarathy & Mohseni 2010; Harimurti *et al.* 2013).

The H$_2$O$_2$-UV process has proven to be effective in degrading ATZ (Beltran *et al.* 1993; Arántegui *et al.* 1995; de Laat *et al.* 1997; Chen *et al.* 2011; Santos 2011; Katsoyiannis *et al.* 2011; Lekkerkerker-Teunissena *et al.* 2012; Wols & Hofman-Caris 2012; Choi *et al.* 2013; Shu *et al.* 2013) but complete mineralization of the molecules is not achieved (Beltran *et al.* 1996; Choi *et al.* 2013). In general, the studies carried out are concerned with: (a) effect of the initial H$_2$O$_2$/ATZ molar ratio, pH, water matrix and radiation intensity on process parameters; (b) the formation and
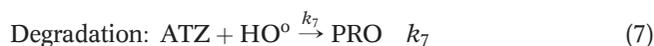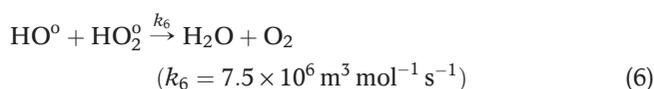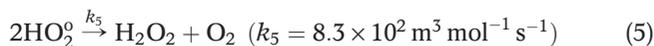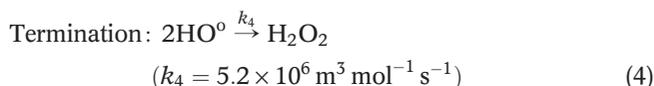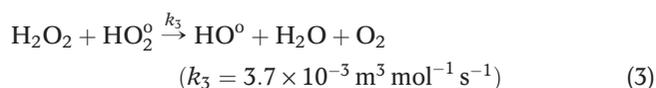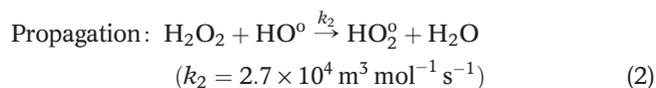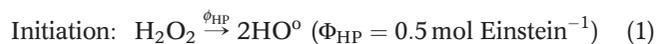
degradation of sub-products; (c) kinetic mechanism; (d) proposition of kinetic rate models mainly assuming pseudo-first order reaction.

Kinetic modelling of photochemical and photocatalytic processes is essential for reactor optimal design, process optimization and scaling-up (Li Puma 2007; Song *et al.* 2008; Lescano *et al.* 2012). For those purposes, the intrinsic reaction kinetics of a pollutant decomposition is required so that the reaction kinetic constants shall be independent of the shape, size and configuration of laboratory reactors. Then, an understanding of the effect of both the degradation pathway and local volumetric rate of photon absorption (LVRPA) on the reaction rate constants is required (Cassano *et al.* 1995; Zalazar *et al.* 2007; Mariani *et al.* 2010). The current work deals with the development of a kinetic model for the degradation of ATZ in aqueous solution using H$_2$O$_2$-UV for design and process optimization purposes. The intrinsic reaction kinetic model developed for degradation of the ATZ using H$_2$O$_2$-UV was based on Lea's reaction scheme for the H$_2$O$_2$ direct photolysis, the hypothesis that unknown ATZ sub-products that absorb UVC radiation are generated during the process, and the general radiative transport equation. The linear spherical source emission (LSSE) model was used to represent the emission of the lamp.

METHODOLOGY

Kinetic model

The proposed reaction scheme for ATZ degradation by H$_2$O$_2$-UV is given by Equations (1) to (9), where reactions 1 to 6 represent Lea's reaction scheme for hydrogen peroxide direct photolysis at 254 nm (Alfano *et al.* 2001), and reactions 7 to 9 represent the decomposition of ATZ into hypothetical unknown products (PRO) which absorb UVC radiation (ATZ is not decomposed by H$_2$O$_2$; Beltran *et al.* 1993).

Initiation: $H_2O_2 \xrightarrow{\phi_{HP}} 2HO^o$ ($\Phi_{HP} = 0.5$ mol Einstein^{-1})   (1)

Propagation: $H_2O_2 + HO^o \xrightarrow{k_2} HO_2^o + H_2O$
$$(k_2 = 2.7 \times 10^4 \, \text{m}^3 \, \text{mol}^{-1} \, \text{s}^{-1}) \quad (2)$$

$H_2O_2 + HO_2^o \xrightarrow{k_3} HO^o + H_2O + O_2$
$$(k_3 = 3.7 \times 10^{-3} \, \text{m}^3 \, \text{mol}^{-1} \, \text{s}^{-1}) \quad (3)$$

Termination: $2HO^o \xrightarrow{k_4} H_2O_2$
$$(k_4 = 5.2 \times 10^6 \, \text{m}^3 \, \text{mol}^{-1} \, \text{s}^{-1}) \quad (4)$$

$2HO_2^o \xrightarrow{k_5} H_2O_2 + O_2$ $(k_5 = 8.3 \times 10^2 \, \text{m}^3 \, \text{mol}^{-1} \, \text{s}^{-1})$ (5)

$HO^o + HO_2^o \xrightarrow{k_6} H_2O + O_2$
$$(k_6 = 7.5 \times 10^6 \, \text{m}^3 \, \text{mol}^{-1} \, \text{s}^{-1}) \quad (6)$$

Degradation: $ATZ + HO^o \xrightarrow{k_7} PRO \quad k_7$ (7)

$ATZ + HO_2^o \xrightarrow{k_8} PRO \quad k_8$ (8)

$ATZ \xrightarrow{\phi_{ATZ}} PRO \quad \Phi_{ATZ}$ (9)

The reaction rate models (Equations (10) and (11)) were obtained by applying both a mass balance to stable species and the pseudo-steady state approach to free-radicals.

$$\mathcal{R}_{ATZ}(r, t) = \phi_{ATZ} e^a_{ATZ}(r, t) - k_{ATZ}(t) C_{ATZ}(t) [e^a_{HP}(r, t)]^{1/2} \quad (10)$$

$$\mathcal{R}_{HP}(r, t) = k_{HP} e^a_{HP,1}(r, t) - k_{HP,1}(t) C_{HP}(t) [e^a_{HP}(r, t)]^{1/2} \quad (11)$$

where k_{ATZ}, $k_{HP,1}$ and $k_{HP,2}$ are kinetic constants (Equations (12) to (14)); e^a_{ATZ} and e^a_{HP} are the local volumetric rate of photon absorption (LVRPA) by ATZ and H$_2$O$_2$, respectively; ϕ_{ATZ} and ϕ_{PH} are ATZ and H$_2$O$_2$ quantum yield; $C_{ATZ}(t)$ and $C_{HP}(t)$ are average concentration of ATZ and H$_2$O$_2$, respectively

$$k_{ATZ} = \frac{(k_7 k_3 + k_8 k_2)(\phi_{HP})^{0.5}}{[k_4 (k_3)^2 + k_5 (k_2)^2 + k_6 k_2 k_3]^{0.5}} \quad (12)$$

$$k_{HP,1} = \frac{k_2 k_3 k_6 \phi_{HP}}{\left[k_4 (k_3)^2 + k_5 (k_2)^2 + k_6 k_2 k_3 \right]^{0.5}} \quad (13)$$

$$k_{HP,2} = \frac{2 k_2 k_3 (\phi_{HP})^{0.5}}{\left[k_4 (k_3)^2 + k_5 (k_2)^2 + k_6 k_2 k_3 \right]^{0.5}} \quad (14)$$

Degradation of pollutants by H$_2$O$_2$-UV is a process where the H$_2$O$_2$ can absorb photons according to two

limiting regimes, fast and slow (Alfano *et al.* 2001). Equation (11) can be simplified as follows:

Fast photon absorption regime: $\mathcal{R}_{HP}(r, t) = -k_{HP,1}\, e^a_{HP}(t)$

$$(15)$$

Slow photon absorption regime:

$$\mathcal{R}_{HP}(r, t) = -k_{HP,2}\, C_{HP}(t)\, [e^a_{HP}(t)]^{1/2} \tag{16}$$

Dynamic concentration profile

A mass balance was applied to ATZ and H$_2$O$_2$. It was assumed that: (a) $V_R/V_T \ll 1$; (b) photoreactor and tank behaved quite closely to a differential reactor and a well-mixed tank, respectively (Silva *et al.* 2013); (c) operation conditions (lamp emission and temperature) were steady state. The resulting model for the dynamic concentration profile and its initial condition are as follows:

$$\left.\frac{dC_i(t)}{dt}\right|_{Tank} = \frac{V_R}{V_T} \langle \mathcal{R}_i(r, t) \rangle_{V_R} \tag{17}$$

$$C_i(O) = C_i^o \tag{18}$$

where i is chemical species (ATZ/H$_2$O$_2$); V_R and V_T are irradiated and tank working volume, respectively; $\langle \mathcal{R}_i(r, t) \rangle_{V_r}$ is the reaction rate averaged over the reactor volume.

Equation (18) was correlated with Equations (10) and (11), giving the following models

$$\left.\frac{dC_{ATZ}(t)}{dt}\right|_{Tank}$$
$$= -\frac{V_R}{V_T}\left\{ \phi_{ATZ}\langle e^a_{ATZ}(r, t)\rangle + k_{ATZ}C_{ATZ}(t)\left[\langle e^a_{HP}(r, t)\rangle\right]^{1/2} \right\} \tag{19}$$

$$\left.\frac{dC_{HP}(t)}{dt}\right|_{Tank}$$
$$= -\frac{V_R}{V_T}\left\{ k_{HP,1}\langle e^a_{HP}(r, t)\rangle + k_{HP,2}C_{HP}(t)\left[\langle e^a_{HP}(r, t)\rangle\right]^{1/2} \right\}$$
$$\langle e^a_i(r, t)\rangle \tag{20}$$

where $\langle e^a_{ATZ}(r, t)\rangle$ and $\langle e^a_{HP}(r, t)\rangle$ are the LVRPA of atrazine and hydrogen peroxide averaged over the reactor volume (Cassano *et al.* 1995).

Local volumetric rate of photon absorption

A rigorous model to account for the spectral specific intensity emitted at 254 nm was obtained by applying the radiative transport equation (Ozisik 1973) to the system (Equation (21)). The following was assumed: (a) steady-state condition; (b) participative and pseudo-homogeneous medium; (c) no emission in the reacting region; (d) monochromatic radiation; (e) uniform absorption coefficients; (f) cylindrical geometry and radiation propagation occurring with azimuthal symmetry

$$\frac{dI_{\lambda,\Omega}(s, \Omega, t)}{ds} + \kappa_{\lambda,i}(t)I_{\lambda,\Omega}(s, \Omega, t) = 0 \tag{21}$$

where $I_{\lambda,\Omega}$ is the monochromatic specific intensity; λ is the wavelength; Ω is the unit vector in the direction of radiation propagation; s is the linear coordinate along the direction Ω; t is the time; $\kappa_{\lambda,i}$ is the linear Naperian absorption coefficient of i species at λ.

Equation (21) with the concepts of inherent radiation field properties, such as incident energy and LVRPA, gives

$$e^a_{\lambda,i}(r, t) = I^o_{\lambda,\Omega}\kappa_{\lambda,i}(t) \int_{\phi 1}^{\phi 2} d\phi \int_{\theta 1}^{\theta 2} \exp\left[-\int_{sr}^{s} \kappa_{\lambda,T}(t)\, ds\right] \operatorname{sen}\theta\, d\theta \tag{22}$$

where θ is the angle formed with the normal axis of the lamp; ϕ is the azumithal angle; $\kappa_{\lambda,T}$ is the exponential Naperian absorption coefficient; sr is the point where the radiation from the lamp arrives at the reactor wall (optical entrance of the reactor); $I^o_{\lambda,\Omega}$ is the boundary condition of Equation (21).

To complete the formulation of the model for LVRPA the following are required (Cassano *et al.* 1995).

(a) Integral limits

$$\theta_1(\phi) = \tan^{-1}\left[\frac{r\cos\phi - (r^2(\cos^2\phi - 1) + R_L^2)^{1/2}}{L_L - z}\right] \tag{23}$$

$$\theta_2(\phi) = \tan^{(-1)}\left[\frac{r\cos\phi - (r^2(\cos^2\phi - 1) + R_L^2)^{1/2}}{-z}\right] \tag{24}$$

$$-\phi_1 = \phi_2 = \cos^{-1}\left[\frac{(r^2 - R_L^2)^{1/2}}{r}\right] \tag{25}$$

where L_L and R_L are the lamp length and radius, respectively.

(b) Boundary condition of Equation (21)

The specific intensity at the optical entrance of the reactor (Equation (26)) must be provided by a lamp emission model which, in this work, was the LSSE model

$$I_{\lambda,\Omega}^{o} = \frac{P_{\lambda,L}}{4\pi L_L} \qquad (26)$$

where $P_{\lambda,L}$ is the lamp power.

(c) Naperian volumetric absorption coefficients

The linear Naperian volumetric absorption coefficient is given as follows:

$$\kappa_{\lambda,i}(t) = \alpha_{\lambda,i} C_i(t) \qquad (27)$$

where $\alpha_{\lambda,i}$ is the molar absorptivity of i species at 254 nm. The exponential Naperian volumetric absorption coefficient at 254 nm is concerned with the reacting mixture formed in the reactor at a given time and, then, is related to the hypothetical unknown sub-products which absorb radiation at 254 nm (Cabrera *et al.* 1997). The Beer–Lambert equation gives

$$\kappa_{\lambda,T}(t) = \alpha_{\lambda,ATZ} C_{ATZ}(t) + \alpha_{\lambda,HP} C_{HP}(t)\alpha_{\lambda,PRO}[C_{ATZ}^{o} - C_{ATZ}(t)] \qquad (28)$$

where $\alpha_{\lambda,ATZ}$, $\alpha_{\lambda,HP}$ and $\alpha_{\lambda,PRO}$ are the molar absorptivity of ATZ, H₂O₂ and PRO, respectively; $C_{ATZ}(t)$, $C_{HP}(t)$ and $[C_{ATZ}^{o} - C_{ATZ}(t)]$ correspond to ATZ, H₂O₂ and PRO concentration at a given time, respectively.

Experimental

Materials

ATZ (98% purity) was provided by Syngenta-Novartis (Brazil). Hydrogen peroxide (35% v/v) was purchased from Nuclear. ATZ solutions were prepared with distilled water. The ATZ was used as supplied.

Equipment, operation conditions and experimental procedure

The process was carried out in an annular photoreactor which is a part of a recycling system (Figure 1). The whole set-up was operated as a closed loop system. The germicidal lamp used was Phillips, model TUV-30 W (output power at 254 nm: 9 W; incident radiant energy at the reactor optical entrance, $G_{ROE} = 1.4 \times 10^{-5}$ Einstein m⁻² s⁻¹). Samples were withdrawn at the tank exit. The operational conditions
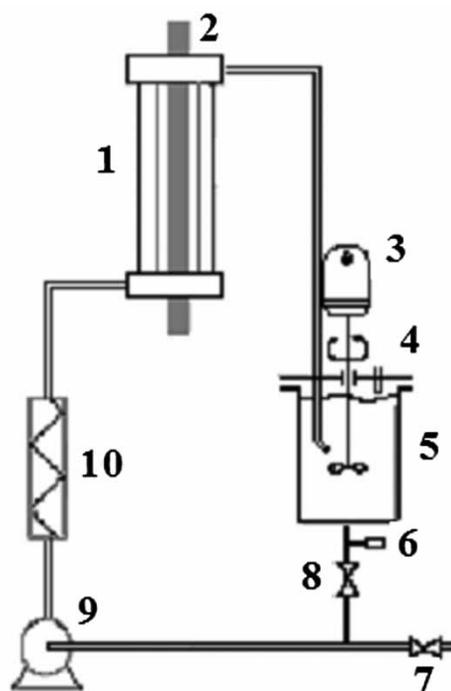

Figure 1 | Experimental set-up (1. photoreactor; 2. lamp; 3. stirrer; 4. feeding port; 5. tank; 6. sample port; 7. drain; 8. valve; 9. pump; 10. condenser).

were: $R = 0$ (initial ATZ concentration: 7.6×10^{-2} mol m⁻³ and 2.2×10^{-2} mol m⁻³); R: 215–578 mol H₂O₂ mol⁻¹ ATZ (initial ATZ concentration: 2.2×10^{-2} mol m⁻³).

The operation procedure was as follows: prior to each degradation run the lamp was turned on for 1,800 s to stabilize its emission. Then, the tank was fed with the ATZ aqueous solution (pH: 6.5; 25 °C) and H₂O₂, the stirrer was turned on (stirring rate: 1,000 rpm), the circulating valve was opened and the pump turned on, allowing the ATZ solution to circulate in the system (flow rate: 5.8×10^{-5} m³ s⁻¹), and, finally, irradiation was started in the photoreactor. Samples of 2.0×10^{-5} m³ were withdrawn at regular intervals of 60 s (UV-H₂O₂, $R = 0$ mol H₂O₂ mol⁻¹ ATZ) and 300 s (H₂O₂-UV, R ranging from 215 to 578 mol H₂O₂ mol⁻¹ ATZ). Dark test runs with H₂O₂ were carried out and sampling was carried out at regular intervals of 60 s. Evolutions of absorbance of the reagent mixture at 254 nm, and concentration of ATZ and H₂O₂ were evaluated along the process.

Analytical analysis

The 254 nm absorbances of ATZ aqueous solution and reacting mixture were measured by spectrophotometry (UV-Vis Cary 17D spectrophotometer). The concentration of ATZ was measured by high performance liquid

chromatography (CG, model 435-B) with UV detector and the C8 Nucleosil column. The mobile phase was an aqueous solution of acetonitrile (40%) and the detection was conducted at 222 nm. The H$_2$O$_2$ concentration was quantified by colorimetry at 350 nm according to Allen *et al*. (1952). The absorption coefficient of the ATZ and reacting mixture were obtained by spectrophotometry, whereas the one concerned with the hypothetical sub-products that absorb radiation was obtained indirectly from Equation (28).

RESULTS AND DISCUSSION

Preliminary degradation studies

In order to degrade the ATZ dissolved in water, experiments were carried out under the following conditions: (a) H$_2$O$_2$ in dark ($R = 215$–578 mol H$_2$O$_2$ mol^{-1} ATZ); (b) H$_2$O$_2$-UV ($R = 0$–578 mol H$_2$O$_2$ mol^{-1} ATZ). It was found that, at the operating conditions of the current work, H$_2$O$_2$ was unable to degrade the ATZ in dark conditions, confirming the results reported by Beltran *et al*. (1993).This herbicide was degraded effectively during illuminated conditions ($R = 0$–578 mol H$_2$O$_2$ mol^{-1} ATZ), indicating that the ATZ was degraded by H$_2$O$_2$-UV by means of synergic actions of oxidation routes, i.e. direct photolysis and direct attack of free-radicals. Results for selected dark and illuminated conditions are shown in Figure 2. A similar trend of results was found for other values of R.

Effect of H$_2$O$_2$-ATZ molar ratio on process efficiency parameters

It is claimed in the literature that the initial concentration of H$_2$O$_2$ affects the H$_2$O$_2$-UV process efficiency parameters
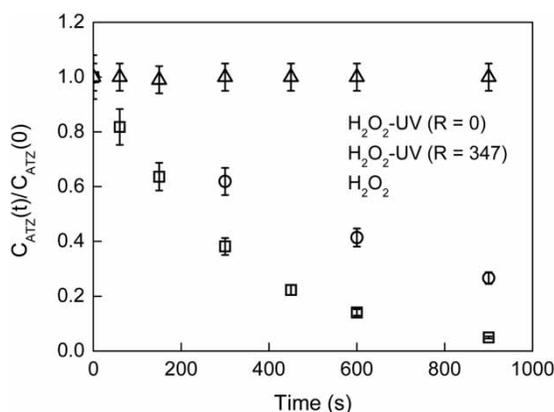
Figure 2 │ ATZ normalized concentration dynamic profiles of selected results.

such as the initial degradation rate and conversion at 300 s (5 min) (Alfano *et al*. 2001). In fact, it is claimed that there is an optimal R (R_{OP}) that leads to maximum values of those parameters. This implies that to carry out the H$_2$O$_2$-UV process using value of R higher than R_{OP} (H$_2$O$_2$ in excess) will not only increase the process costs and decrease the rate of the pollutant removal but also leave a high residual of H$_2$O$_2$ in the treated water (Crittenden *et al*. 1999).

The current work is concerned with the kinetic modelling of the ATZ degradation process via H$_2$O$_2$-UV when R is the optimal for a given ATZ initial concentration (2.2×10^{-2} mol m^{-3}) and the incident radiant energy at the reactor optical entrance is 1.4×10^{-5} Einstein m^{-2} s^{-1}.

The effect of the initial H$_2$O$_2$/ATZ molar ratio on the process parameters has been investigated (Table 1). The optimal value found for the initial molar ratio seems to be 347 mol H$_2$O$_2$ mol^{-1} ATZ (Table 1) as at this molar ratio the initial degradation rate and conversion at 300 s were, respectively, 83% and 77% higher than those found for $R = 0$ (direct photolysis process). The existence of an R_{OP} might be explained by the fact that at $R < R_{OP}$ the H$_2$O$_2$ absorbs only a small fraction of the incident radiation energy, leading to low values of ATZ initial rate and conversion at 300 s. At $R > R_{OP}$, however, H$_2$O$_2$ becomes a stronger scavenger of hydroxyl radical, competing with ATZ, and leading to a decrease in the values of initial ATZ degradation rate and conversion at 300 s.

Energy requirement and operation costs

The economic feasibility of the H$_2$O$_2$-UV process are associated with: (a) investments costs in equipment; (b) operating and maintenance costs (electrical power requirement), which depend on the nature of the water to be treated and operating condition applied. One of the most significant obstacles to the application of AOPs is energy consumption. Bolton *et al*. (1998) have proposed the concept of electrical energy per order ($E_{E/O}$) to determine the energy requirement for 90% removal of a pollutant in 1.0 m^3 of water. The $E_{E/O}$ (Equation (29)) is based on the assumption that

Table 1 │ Effect of initial molar rate on efficiency parameters

R (mol H$_2$O$_2$ mol^{-1} ATZ)	$C_{ATZ}^0 \times 10^2$ (mol m^{-3})	$\langle \mathcal{R}_{ATZ}^0 \rangle$ (mol m^{-3} s^{-1})	$X_{300\,s}$ (%)
0	2.2	7.0	14.3
215	2.2	34.0	58.0
347	2.2	41.0	63.0
578	2.2	29.0	58.0

the pollutant concentration is low and its decay follows pseudo-first order kinetics. $E_{E/O}$ acceptable values are smaller than 10 kWh m^{-3} order^{-1} (Shu et al. 2013)

$$E_{E/O} = \frac{1000 \, P \, t_{90\%}}{60 \, V \, Ln[C_{ATZ}^{o}/C_{ATZ}^{t_{90\%}}]} \qquad (29)$$

where P is the power of the lamp (W); $t_{90\%}$ is the time required for achieving ATZ removal of 90% (s); V is the volume (m^3) $C_{ATZ}^{t_{90\%}}$ is the ATZ concentration equivalent to 90% of removal (mol m^{-3}).

According to Cassano et al. (1995), AOPs, such as H_2O_2-UV, do not present a pseudo-first order kinetics since its reaction rate depends on the LVRPA. (This process parameter depends on the concentration of pollutant by means of the Naperian absorption coefficient.) Nevertheless, it is interesting to analyse the process according to the parameter $E_{E/O}$ since this analysis gives preliminary information about process energy requirement. However, it must be taken into consideration that the economic analysis based on the concept of $E_{E/O}$ is limited as the $E_{E/O}$ is an overall parameter with limited phenomenological value. Based on that, a rough economic analysis is presented in this work. Values of ATZ pseudo-first order constant ($k_{ATZ,P}$), $E_{E/O}$ and treatment costs (energy cost, E_{EC}, and H_2O_2 solution preparation cost, E_{HPC}) were calculated for conditions where R values were 0.0 mol H_2O_2 mol^{-1} ATZ and $R = 347.0$ mol H_2O_2 mol^{-1} ATZ (Table 2).

Small values of $E_{E/O}$ indicate a more efficient process since less energy is required for achieving a fixed drop (90%) in concentration of the pollutant. The results obtained have shown how appreciably the addition of H_2O_2 to the system at the optimal R impacted positively the decomposition of ATZ, and this can be summarized as: (a) the time required for removing 90% of ATZ was 87.7% smaller; (b) the $k_{ATZ,P}$ increased to 89%; (c) the $E_{E/O}$ decreased to 91%; (d) the energy cost for the ATZ removal of 90% in 1.0 m^3 of water decreased to 90.6%. Similar results were reported by Behnajady et al. (2009) who claimed that $E_{E/O}$ can be minimized by increasing the H_2O_2 pollutant molar ratio up to the optimum value. However, treatment costs

increase due to the costs of H_2O_2. In the case of this work, US$1.0 must be added to the energy cost analysis for each m^3 of water due to the costs of H_2O_2 for the optimal condition, $R = 347.0$ mol H_2O_2 mol^{-1} ATZ (Table 2).

Kinetic modelling

Naperian molar absorption coefficient

The values of Naperian molar absorption coefficients of ATZ, ATZ sub-products and H_2O_2 at 254 nm (α_{PRO}) are required for elucidating the kinetics of the degradation ATZ by H_2O_2-UV, as the degradation rate depends on LVRPA, which depends on those coefficients. The obtained value of $\alpha_{\lambda,ATZ}$ was 552.7 m^2 mol^{-1}. This value is in agreement with that reported by Beltran et al. (1993). The value of α_{λ,H_2O_2} (3.7 m^2 mol^{-1}) was obtained from literature (Beltran et al. 1993). The value of α_{PRO} was evaluated according to Cabrera et al. (1997) and was equal to 469.9 m^2 mol^{-1}.

Kinetic parameter estimation and model validation

Estimations of the ATZ direct photolysis quantum yield at 254 nm (ϕ_{ATZ}) and kinetic parameters for the H_2O_2-UV process (k_{ATZ}; $k_{PH,1}$; $k_{PH,2}$) were calculated using data obtained for the conditions where R varied in the range of 0.0–578.0 mol H_2O_2 mol^{-1} ATZ. The kinetic model developed comprised Equations (19), (21) and (22). The resulting equation system was solved numerically using the multiparameter algorithm (Runge–Kutta method) coupled with an optimization routine (Levenberg–Marquard method). Firstly the equation system was solved for the direct photolysis process ($R = 0$) in order to estimate the value of ATZ quantum yield. (This parameter is required during the estimating of the H_2O_2-UV kinetic parameters.) Then, it was solved for the H_2O_2-UV process ($R > 0$). The values found for ϕ_{ATZ}, k_{ATZ}, $k_{PH,1}$ and $k_{PH,2}$ were 0.048 mol Einstein^{-1}, 7.40 (m^3 Einstein^{-1} s^{-1})$^{1/2}$, 0.00 mol Einstein^{-1} and 1.58 (m^3 Einstein^{-1} s^{-1})$^{1/2}$, respectively.

Table 2 | Energy requirement and operation costs

R (mol H_2O_2 mol^{-1} ATZ)	$t_{90\%}$ (s)	$k_{ATZ,p}$ (s^{-1})	$E_{E/O}$ (kWh m^{-3} order^{-1})	E_{EC}^{a} (US$ kWh^{-1} m^{-3})	E_{HPC}^{a} (US$ m^{-3})
0.0	4,860.0	5.2×10^{-3}	1.51	0.18	0.00
347.0	600.0	4.3×10^{-2}	0.14	0.02	1.00

[a]The unit prices for H_2O_2 (US$4.14 kg^{-1}) and electrical energy (US$0.12 kWh^{-1}) were based on Brazilian economy.
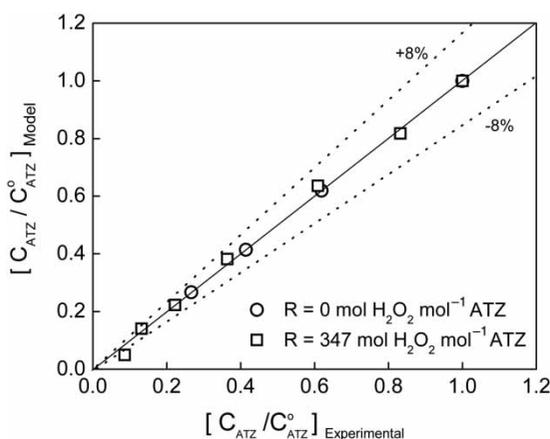
Figure 3 | Model predictions versus data for selected experiments.

The kinetic rate models for ATZ and H_2O_2 are given by Equations (30) to (32), respectively. Those results suggested that the decomposition of ATZ by H_2O_2-UV has the following features: (a) ATZ is decomposed mainly by free-radical attack (95.2%) as its primary quantum yield is rather low (4.8%); (b) H_2O_2 direct photolysis reaction assumes a limiting case where the LVRPA is quite low, as its rate was found to be directly proportional to the H_2O_2 concentration and the square root of the LVRPA (Alfano *et al.* 2001)

$$R = 0 \quad \mathcal{R}_{ATZ}(r, t) = -0.048 \, e^a_{ATZ}(r, t) \tag{30}$$

$$
\begin{aligned}
R = 215 - 578 \; \mathcal{R}_{ATZ}(r, t) \\
= -0.048 \, e^a_{ATZ}(r, t) - 7.4 \, C_{ATZ}(t)[e^a_{HP}(r, t)]^{0.5}
\end{aligned}
\tag{31}
$$

$$\mathcal{R}_{ATZ}(r, t) = -1.58 C_{HP}(t) \, [e^a_{HP}(r, t)]^{0.5} \tag{32}$$

Once the kinetic parameters had been obtained and the reaction rate model formulated completely, the model prediction could be made. The model fits the data of all conditions tested with an accuracy ranging from 90 to 98%. The comparison between data and simulation values for selected experiments ($R = 0$ and $R = R_{OP}$) is shown in Figure 3. The results indicate that the model developed from simple kinetic formulation is able to produce intrinsic kinetic results and is adequate for photoreactor design purposes (Cabrera *et al.* 1997; Mariani *et al.* 2010).

CONCLUSION

The main conclusions drawn from this study are as follows: (a) the decomposition of ATZ by H_2O_2-UV takes place by the synergetic actions of oxidation routes: direct photolysis of ATZ and free-radical attack to ATZ molecules; (b) the addition of H_2O_2 impacts the efficiency of ATZ removal from a system irradiated with UVC light; (c) there is an optimal H_2O_2/ATZ molar ratio for a given condition, which leads the ATZ removal and maximizes process efficiency, leading to minimum energy consumption; (d) the quantum yield of ATZ is low; (e) H_2O_2 direct photolysis assumes a limiting case where the LVRPA is rather low; (f) the model represents the intrinsic kinetics, fits well to the data and is adequate for design purpose.

REFERENCES

Alfano, O. M., Brandi, R. & Cassano, A. 2001 Degradation kinetics of 2,4-D in water employing hydrogen peroxide and UV radiation. *Chemical Engineering Journal* **82**, 209–218.

Allen, A. O., Hochanadel, C., Ghormley, J. & Davis, T. 1952 Decomposition of water and aqueous solution under mixed fast neutron and gamma radiation. *Journal of Physical Chemistry* **56**, 575–586.

Arántegui, J., Prado, J., Chamrro, E. & Esplugas, S. 1995 Kinetics of the UV degradation of atrazine in aqueous solution in the presence of hydrogen peroxide. *Journal of Photochemistry and Photobiology A: Chemistry* **88**, 65–74.

Behnajady, M. A., Vahid, B., Modirshahla, N. & Shokri, M. 2009 Evaluation of electrical energy per order (E_{EO}) with kinetic modeling on the removal of Malachite Green by US/UV/H_2O_2 process. *Desalination* **249**, 99–103.

Beltran, F. J., Gonzalez, M. & Alvarez, P. 1996 Aqueous UV radiation and UV/H_2O_2 oxidation of atrazine first degradation products: deethylatrazine and deiso-propylatrazine. *Environmental Toxicology and Chemistry* **15**, 868–872.

Beltran, F. J., Ovejero, G. & Acedo, B. 1993 Oxidation of atrazine in water by ultraviolet radiation combined with hydrogen peroxide. *Water Research* **27**, 1013–1021.

Bolton, J. R., Valladares, J., Zanin, J., Cooper, W., Nickelsen, M., Kajdi, D., Waite, T. & Kurucz, C. 1998 Figures-of-merit for advanced oxidation technologies: a comparison of homogeneous UV/H_2O_2, heterogeneous TiO₂ and electron beam processes. *Journal of Advanced Oxidation Technologies* **3**, 174–181.

Brasil Portaria N° 2914. 2012 *Ministério da Saúde (Ministry of Health Ordinance 2914)* Publicada no Dário Oficial (da Republica Federativa do), Brasil, no. 3 de 04/01/2012, Seção 1, pagina 43.

Cabrera, M. I., Martín, C., Alfano, O. & Cassano, A. 1997 Photochemical decomposition of 2,4-dichlorophenoxyacetic acid (2,4-D) in aqueous solution. I. Kinetic study. *Water Science and Technology* **35**, 31–39.

Cassano, A. E., Martín, C., Brandi, R. & Alfano, O. 1995 Photoreactor analysis and design: Fundamentals and applications. *Industrial & Engineering Chemistry Research* **34**, 2155–2201.

Chen, H., Bramanti, E., Longo, I., Onor, M. & Ferrari, C. 2011 Oxidative decomposition of atrazine in water in presence of hydrogen peroxide using an innovative microwave photochemical reactor. *Journal of Hazardous Material* **186**, 1808–1815.

Choi, H., Kim, D. & Lee, T. 2013 Photochemical degradation of atrazine in UV and UV/H₂O₂ process: pathways and toxic effects of products. *Journal of Environmental Science and Health, Part B: Pesticides, Food Contaminants and Agricultural Wastes* **48** (11), 927–934.

Crittenden, J. C., Hu, S., Hand, W. & Green, A. 1999 A kinetic model for H₂O₂/UV process in a completely mixed batch reactor. *Water Research* **33** (10), 2315–2328.

de Laat, J., Berger, P., Poinot, T., Karpel vel Leitner, N. & Doré, M. 1997 Modeling the oxidation of atrazine by H₂O₂/UV. Estimation of kinetic parameters. *Ozone Science and Engineering* **19**, 395–408.

Harimurti, S., Rahmah, A. & Omar, A. 2013 Kinetics of methyldiethanolamine mineralization by using UV/H₂O₂ process. *Clean-Soil, Air, Water* **41** (12), 1165–1174.

Kassinos, D., Varnaki, N., Michael, C. & Piera, P. 2009 Homogeneous oxidation of aqueous solutions of atrazine and fenitrothion through dark and photo-Fenton reactions. *Chemosphere* **74**, 866–872.

Katsoyiannis, I. A., Canonica, S. & von Gunten, U. 2011 Efficiency and energy requirements for the transformation of organic micropollutants by ozone, O₃/H₂O₂ and UV/H₂O₂. *Water Research* **45** (13), 3811–3822.

Lekkerkerker-Teunissena, K., Benottic, M., Snyderc, S. & Dijk, H. 2012 Transformation of atrazine, carbamazepine, diclofenac and sulfamethoxazole by low and medium pressure UV and UV/H₂O₂ treatment. *Separation and Purification Technology* **96** (21), 33–42.

Lescano, M., Zalazar, C., Cassano, A. & Brandi, R. 2012 Kinetic modeling of arsenic (III) oxidation in water employing the UV/H₂O₂ process. *Chemical Engineering Journal* **211–212**, 360–368.

Li Puma, G., Toepfer, B. & Gora, A. 2007 Photocatalytic oxidation of multicomponent systems of herbicides: scale-up of laboratory kinetics rate data to plant scale. *Catalysis Today* **124** (3–4), 124–132.

Mariani, M. L., Labas, M., Brandi, R., Cassano, A. & Zalazar, C. 2010 Degradation of a mixture of pollutants in water using the UV/H₂O₂ process. *Water Science and Technology* **61** (12), 3026–3032.

Ozisik, M. N. 1973 *Radiative Transfer Interactions with Conduction and Convection*. Wiley, New York.

Santos, B. S. 2011 Avaliação do processo H₂O₂/UV como pós-tratamento e remoção da atrazina de um efluente secundário de ete para fins de reuso (Evaluation of the H₂O₂/UV process as post-treatment and atrazine removal from the secondary effluent of an ETE for effluent reuse). PhD thesis, UFRJ/COPPE, Rio de Janeiro, Brazil.

Sarathy, S. & Mohseni, M. 2010 Effects of UV/H₂O₂ advanced oxidation on chemical characteristics and chlorine reactivity of surface water natural organic matter. *Water Research* **44**, 4087–4096.

Silva, A. B., Lima Filho, N., Palha, M. & Sarmento, S. 2013 Kinetics of water disinfection using UV-C radiation. *Fuel* **114–123**.

Shu, Z., Bolton, J. R., Belosevic, M. & El Din, M. G. 2013 Photodegradation of emerging micropollutants using the medium-pressure UV/H₂O₂ advanced oxidation process. *Water Research* **47**, 2881–2889.

Song, W., Ravindran, V. & Pirbarazi, M. 2008 Process optimization using a kinetic model for the ultraviolet radiation-hydrogen peroxide decomposition of natural and synthetic organic compounds in groundwater. *Chemical Engineering Science* **63** (12), 3249–3270.

Wols, B. A. & Hofman-Caris, C. 2012 Review of photochemical reaction constants of organic micropollutants required for UV advanced oxidation processes in water. *Water Research* **46** (9), 2815–2827.

Yue, P. 1993 Modelling kinetics and reactor for water purification by photo-oxidation. *Chemical Engineering Science* **48**, 1–11.

Zalazar, C. S., Lovato, M., Labas, M., Brandi, R. & Cassano, A. 2007 Intrinsic kinetics of the oxidative reaction of dichloroacetic acid employing hydrogen peroxide and ultraviolet radiation. *Chemical Engineering Science* **62**, 5840–5853.